Letters

A Simple Autonomous Phase-Shifting PWM Approach for Series-Connected Multi-Converter Harmonic Mitigation

Liyang Du and Jinwei He

***Abstract*—In order to reduce the high-frequency switching harmonics of cascaded H-bridge (CHB) converters, phase-shifting pulsewidth modulation (PWM) using a centralized controller has been extensively studied. In this letter, an improved decentralized PWM strategy is proposed as an alternative approach for decentralized modulation. First, the output current of CHB converter is measured by each power cell as an effective synchronization indicator to identify the digital carrier angle of each power cell at the exact time of output current fundamental component zero crossing. Then, a PI controller dynamically adjusts the carrier relative angles of all power cells until they are properly interleaved. Together with the an inverse power factor droop for power sharing control, a CHB converter system can operate at autonomous islanded mode in a fully decentralized manner. Experiments from a single phase islanded CHB converter have been conducted to validate the correctness of the proposed approach.**

***Index Terms*—Autonomous control, cascaded H-bridge, inverse droop control, phase-shifting modulation, power quality.**

I. Introduction

DISTRIBUTED dc resources including photovoltaics and batteries are widely used to power up ac loads or integrated into high-voltage main grids in a collaborative manner [1], [2]. In the previous research, parallel operation of distributed generation (DG) units has been extensively studied and the real power frequency droop control and the reactive power voltage magnitude droop control have been widely used to facilitate the power sharing requirement in a decentralized manner [3].

For high-voltage grid integration, bulky matching transformers are needed for low-voltage DG units. Alternatively, cascaded H-bridge (CHB) converter for transformer-less grid integration has received increasing attentions due to its modular configuration and the multiple dc ports to interconnect low-voltage distributed dc resources with different features [4]. Regarding the modulation approach of CHB converters, phase-shifting modulation has been widely adopted to reduce the impact of switching frequency harmonic components. A central controller is usually needed for its closed-loop control and pulsewidth modulation (PWM) generation [4]–[6]. However, centralized architectures are associated with low reliability, particularly for high-voltage applications that need more power cells.

In addition, for the emerging applications that interconnect remotely installed distributed DG resources to form a cascaded power-cells-based electrical system, using a centralized control is difficult as sending PWM gating signals from central controller to power cells via long signal wires are particularly sensitive to disturbances and noises. To deal with this problem, the inverse power factor or inverse real power droop control can be applied to the system [7]. Accordingly, multiple series-connected power cells can actively participate in the sharing of load demand without any communications between them. Although the power sharing is performed in a decentralized manner, it should be noted that the carriers for PWM gating are generated independently by the local digital processors of power cells. As a result, bulky *LC* filters are needed to filter output the impact of excessive harmonic components of the CHB converter output voltage. Although a few literatures have discussed the phase-shifting PWM using coordinated power cell local controllers [8], but cost-expensive high bandwidth communications between power cells with low delay are always needed.

In this letter, a phase-shifting PWM of CHB converter is realized by using only local control of each power cell. First, the fundamental component of output current is extracted by each power cell local controller and the zero-crossing time is utilized as the base point to identify the carrier angle of each power cell. Afterward, an online phase-shifting modulation tuning is applied with the adjustment of carrier phase angles. The proposed decentralized phase-shifting PWM approach has been validated on a single-phase islanded system as an example. It has also been demonstrated that the modulation approach has no obvious interference with the decentralized power sharing control.

II. Proposed Method

A fully autonomous phase-shifting PWM approach for single-phase islanded CHB converter is proposed in this section.

Manuscript received April 16, 2019; revised May 10, 2019; accepted May 22, 2019. Date of publication May 27, 2019; date of current version September 6, 2019. This work was supported in part by the National Key Research and Development Program of China under Grant 2017YFB0902001 and in part by Inner Mongolia Science Technology Program "Study on the integration of technology and economy system for renewable energy microgrid." *(Corresponding author: Jinwei He.)*

The authors are with the School of Electrical and Information Engineering, Tianjin University, Tianjin 300072, China (e-mail: du_liyang@126.com; jinwei.he@tju.edu.cn).

Color versions of one or more of the figures in this letter are available online at http://ieeexplore.ieee.org.

Digital Object Identifier 10.1109/TPEL.2019.2919386

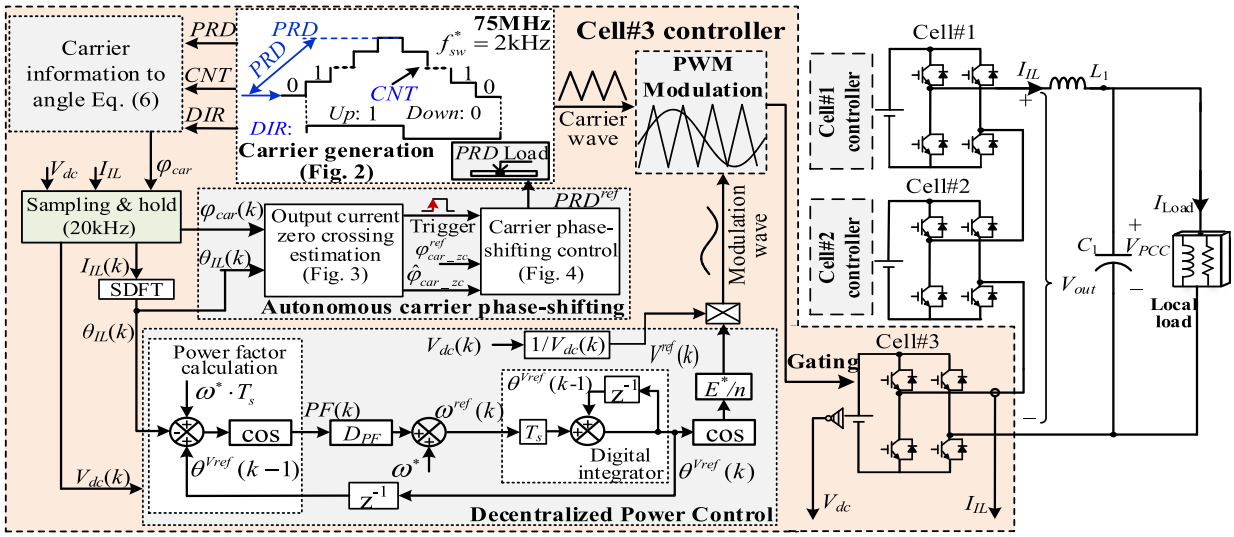

Fig. 1. Diagram of CHB converter with the proposed decentralized controller.

A. System Configuration

The diagram of a CHB converter is shown in Fig. 1. The power circuit is composed of a single-phase CHB converter and an output *LC* filter (L_1 andC_1). The filter capacitor voltage $V_{\rm PCC}$ is regulated to supply the local load with current $I_{\rm load}$. In order to focus on the power control and PWM control of the CHB converter, it is assumed that all power cells have ideal voltage source in the dc rail.

As there is no central controller in this system, all power cell local controllers have the same control architecture. The proposed autonomous controller of a power cell in CHB is shown in the left part of Fig. 1. The details are presented in the following sections.

B. Decentralized Power Control

For the sake of simplicity, all power cells are assumed to provide the same real and reactive power to local loads. A simple inverse power factor droop control is adopted to realize the aforementioned control target as

$$\omega^{\rm ref}(k) = \omega^* + {\rm PF}(k) \cdot D_{\rm PF} \tag{1}$$

where $\omega^{\rm ref}(k)$ is the angular frequency of reference voltage, and ω^* is the nominal angular frequency. ${\rm PF}(k)$ is the estimated power factor of the power cell, and $D_{\rm PF}$ is the inverse droop coefficient. *k* means the sampled values at the *k*th sampling interval.

With the obtained angular frequency, the reference voltage angle $\theta^{V\,{\rm ref}}(k)$ can be given using a digital integrator as

$$\theta^{V\,{\rm ref}}(k) = \theta^{V\,{\rm ref}}(k-1) + \omega^{\rm ref}(k) \cdot T_s \tag{2}$$

where $\theta^{V\,{\rm ref}}(k-1)$ is the reference voltage angle in the previous sampling period, and T_s is the processing period of the power cell.

Then, the instantaneous reference voltage $V^{\rm ref}(k)$ is calculated as

$$V^{\rm ref}(k) = E^*/n \cdot \cos(\theta^{V\,{\rm ref}}(k)) \tag{3}$$

where E^* is the nominal value of point of common coupling (PCC) voltage, and *n* is the series-connected power cell numbers.

As the output voltage of a power cell is high-frequency PWM waveform, an accurate measurement of output voltage for power factor calculation is difficult. When only the output current $I_{IL}(k)$ is measured to carry out the inverse power factor droop control as shown in (1), the power factor of a power cell can be estimated using the following two steps. First, the output current angle $\theta_{IL}(k)$ ranging from $-\pi$ to π rad is extracted using a sliding discrete fourier transform extractor. Then, the power factor of power cell is simply estimated as

$${\rm PF}(k) = \cos(\theta^{V\,{\rm ref}}(k) - \theta_{IL}(k)). \tag{4}$$

To solve the algebraic-loop problems associated with the implementation of (4), it is modified by using the reference voltage angle of previous sampling period as

$${\rm PF}(k) = \cos(\theta^{V\,{\rm ref}}(k-1) + \omega^* \cdot T_s - \theta_{IL}(k)). \tag{5}$$

With the implementation of the inverse droop control, the reference voltage of all power cells has the same phase angle to equally share the load demand.

C. Decentralized Phase-Shifting Modulation

1) Carrier Angle Estimation: It is well understood that the phase-shifting PWM of a CHB converter is realized by the proper shifting of power cells carrier angle $\varphi_{\rm car}$, according to power cell numbers. This needs to identify the relative carrier phase angle between power cells. However, as there is no control center in this proposed system, it is impossible for a power cell to acquire the carrier information of other power cells. Alternatively, it is observed that all power cells have the same output current even

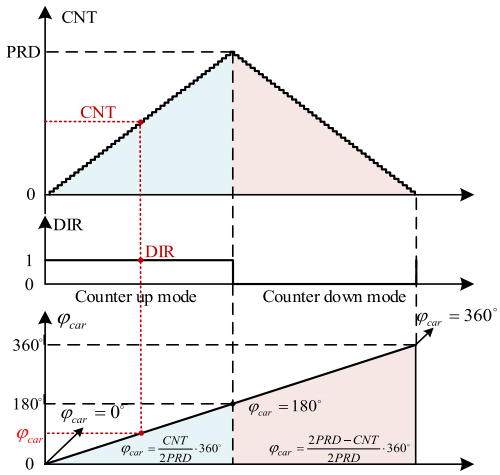

Fig. 2. Illustration of carrier counters in up and down mode.

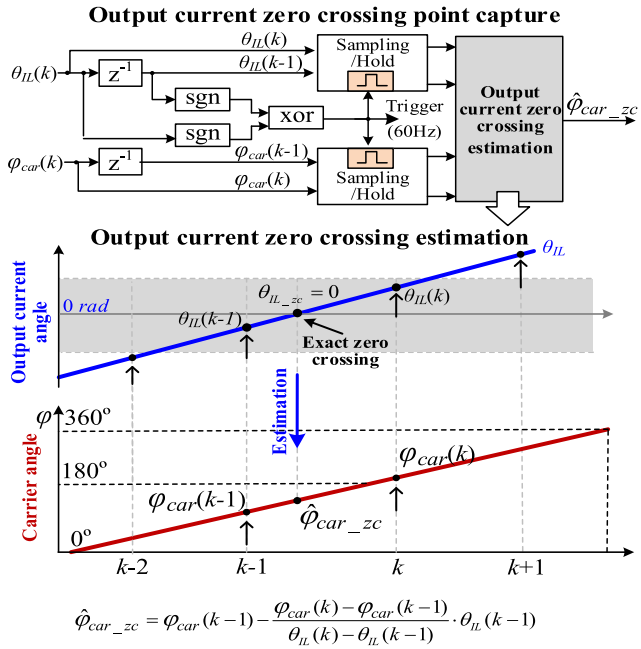

$$\hat{\varphi}_{car\_zc}=\varphi_{car}(k-1)-\frac{\varphi_{car}(k)-\varphi_{car}(k-1)}{\theta_{IL}(k)-\theta_{IL}(k-1)}\cdot\theta_{IL}(k-1)$$

Fig. 3. Diagram of the output current zero-crossing estimation.

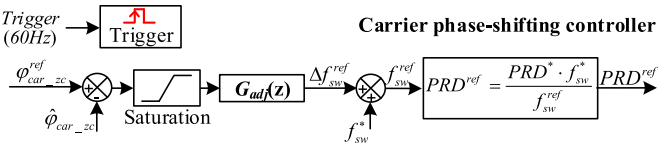

Fig. 4. Diagram of the carrier phase-shifting controller.

when they are far away from each other. This finding is utilized as a common synchronizer for the identification of relative phase angle of power cell carriers.

First, a high-resolution digital counter with 75 MHz digital clock is operating in up and down mode to generate the triangle carrier at 2 kHz nominal switching frequency $f^{*}_{\rm sw}$. The nominal period register $\rm PRD^{*}$ is simply set to 18 750 (75 MHz/2 kHz/2) for the system as shown in Fig. 1. When the clock counts, the process of a digital is shown in Fig. 2, where CNT is the instantaneous counter value register. DIR is the counter direction flag bit, which is 1 when the digital counter is in counter up mode and 0 in counter down mode [9]. From Fig. 2, it is easy to obtain that the digital expression of the counter can be converted into the carrier phase angle $\varphi_{\rm car}$ as

$$\varphi_{\rm car}=\frac{\rm Abs(2PRD-DIR\cdot 2PRD-CNT)}{\rm 2PRD}\cdot 360^{\circ} \quad (6)$$

where the operator "Abs" is a function to obtain the absolute value.

Then, the digital carrier phase angle can be captured at the time instant of fundamental component output current zero crossing. However, note that even the $\theta_{IL}(k)$ is extracted at a relatively high frequency at 20 kHz, it is still difficult to get a sample with $\theta_{IL}=0$. In order to overcome this limitation, a simple interpolation method is applied to estimate the carrier phase angle at the exact time with $\theta_{IL}=0$.

The diagram of carrier phase angle estimation is shown in Fig. 3. First, the two adjacent output current phase angles $\theta_{IL}(k-1)$ and $\theta_{IL}(k)$ that are close to the zero-crossing point are captured as shown in the top of Fig. 3. The phase angle of the carrier at $k-1$th and kth sampling interval are captured as $\varphi_{\rm car}(k-1)$ and $\varphi_{\rm car}(k)$. Due to that both the phase angles of digital carrier and output current have good linearity in a short time interval as shown in Fig. 3, the following relationship is obtained:

$$\frac{\hat{\varphi}_{\rm car\_zc}-\varphi_{\rm car}(k-1)}{\theta_{IL\_zc}-\theta_{IL}(k-1)}=\frac{\varphi_{\rm car}(k)-\varphi_{\rm car}(k-1)}{\theta_{IL}(k)-\theta_{IL}(k-1)}. \quad (7)$$

Afterward, as $\theta_{IL\_zc}=0$ represents the exact zero-crossing current phase angle, the carrier angle at the time instant of output current phase angle zero crossing is estimated as

$$\hat{\varphi}_{\rm car\_zc}=\varphi_{\rm car}(k-1)-\frac{\varphi_{\rm car}(k)-\varphi_{\rm car}(k-1)}{\theta_{IL}(k)-\theta_{IL}(k-1)}\cdot\theta_{IL}(k-1) \quad (8)$$

where $\hat{\varphi}_{\rm car\_zc}$ is the estimated angle of carrier.

2) Carrier Phase-Shifting Control: For a CHB converter system, the preferred carrier phase angle $\varphi^{\rm ref}_{\rm car\_zc}$ of each power cell at the time instant of output current zero crossing can be pre-determined in an interleaved manner. Then, as shown in Fig. 4, the difference between the preferred carrier phase angle $\varphi^{\rm ref}_{\rm car\_zc}$ and the estimated carrier phase angle $\hat{\varphi}_{\rm car\_zc}$ is adopted to carry out the reference switching frequency $\Delta f^{\rm ref}_{\rm sw}$ tuning as

$$\begin{aligned}\Delta f^{\rm ref}_{\rm sw}&=G_{\rm adj}(z)\cdot(\varphi^{\rm ref}_{\rm car\_zc}-\hat{\varphi}_{\rm car\_zc})\\&=(k_p+\frac{k_i}{s})\cdot(\varphi^{\rm ref}_{\rm car\_zc}-\hat{\varphi}_{\rm car\_zc})_{s=\frac{2}{T_{s,60\ \rm Hz}}\times\frac{z-1}{z+1}}\end{aligned} \quad (9)$$

where k_p and k_i are the proportional and integral gain of the frequency regulator, respectively. $\Delta f^{\rm ref}_{\rm sw}$ is the reference carrier frequency deviation. Note that the abovementioned regulator is only performed once in each fundamental cycle. In addition, the PI regulator has small gains to slowly adjust the deviation of carrier frequency. Furthermore, consider that the switching

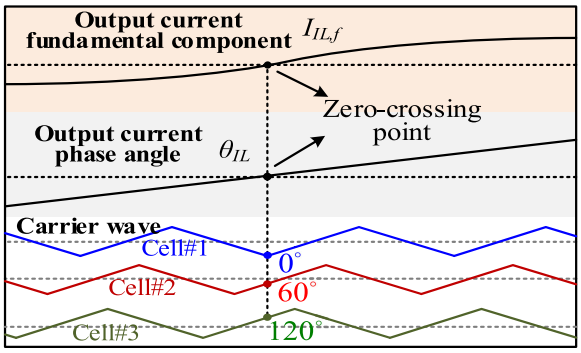

Fig. 5. Illustration of the carrier arrangement versus the output current zero-crossing point.

TABLE I
PARAMETERS OF THE SYSTEM

System parameters	
Rated PCC voltage	Single-phase 120VRMS/60 Hz
DC link voltage	80V (for Cell#1~ Cell#3)
Circuit parameters	
LC filter	L_1=1mH; R_1=0.1Ω; C_1=40uF
PCC load	DG1: L_{load}=1mH; R_{load}=27Ω
Switching frequency of power cells	2 kHz
Control parameters	
Inverse power factor droop controller	D_{PF}=1.4 rad/s (for Cell#1~ Cell#3)
Phase-shifting PI controller	k_p=0.080 Hz/deg; k_i=0.002 Hz/(deg·s)

frequency is inverse proportional to the carrier period register PRD as

$$\frac{f_{\rm sw}^*}{\Delta f_{\rm sw}^{\rm ref}+f_{\rm sw}^*}=\frac{\rm PRD^{ref}}{\rm PRD^*} \tag{10}$$

where $f_{\rm sw}^*$ is the nominal switching frequency, and $\rm PRD^*$ is the register value corresponding to nominal switching frequency. Then, it is easy to obtain the reference $\rm PRD^{ref}$ as

$$\rm PRD^{ref}=(PRD^*\cdot f_{sw}^*)/(f_{sw}^*+\Delta f_{sw}^{ref}). \tag{11}$$

With the adoption of the proposed adaptive carrier adjustment method, the carriers of a CHB converter with three power cells are illustrated in Fig. 5, where the carrier angles of power cells are 0°, 60°, and 120°, respectively, at the output current zero crossing.

III. VERIFICATIONS

The proposed method has been experimentally tested on a down-scale laboratory prototype as shown in Fig. 1. The key circuitry and control parameters can be seen from Table I. The experiment has three stages with different control modes. At stage 1, all power cells are controlled independently with random reference voltage initial phase angles. Nevertheless, in order to make the comparison more straightforward, the carrier angles of all power cells are controlled to be the same using the proposed method at stage 1. At stage 2, only the inverse power factor droop control is activated. Finally, both inverse power factor droop control and the phase-shifting PWM control are applied to the system at stage 3.

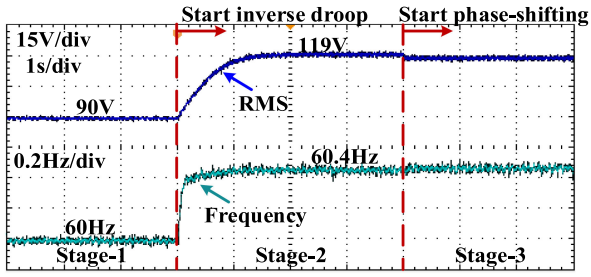

Fig. 6. RMS value and frequency performance of PCC voltage.

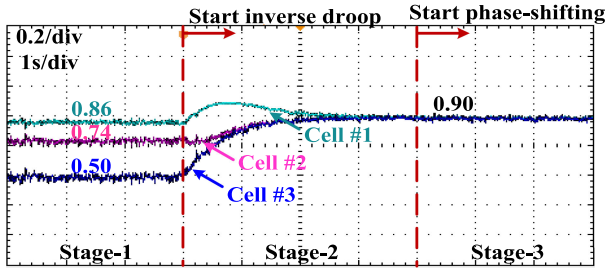

Fig. 7. Power factor performance of three power cells.

First, the rms value and frequency of PCC voltage are shown in Fig. 6. At stage 1, it is clearly seen that the rms value is only 90 V and the frequency is fixed 60 Hz, due to the random reference voltage angles of three power cells. At stage 2, the PCC voltage magnitude restores to 119 V when the inverse power factor droop control is applied. However, there appears slight frequency variations to 60.4 Hz at stage 2. Finally, when the phase-shifting PWM control is also applied to the system at stage 3, the voltage magnitude and the frequency of PCC voltage are roughly unchanged.

The power factors of three power cells are shown in Fig. 7. Due to the impact of random reference voltage angles of three power cells at stage 1, power factors of three power cells are 0.86, 0.74, and 0.5, respectively. At stage 2, the inverse droop control is activated, and it is seen that the power factors of three power cells become the same at around 0.90. Similarly, at stage 3, the power factors of three power cells keep the same value.

The detailed voltage and current waveforms at different stages are shown in Fig. 8. First, Fig. 8(a) shows the output voltage of cascaded power cells, PCC voltage, output current, and load current at stage 1, where it is seen that the PCC voltage is high distorted as the output voltage is irregular multi-level PWM waveforms depending on the phase angle relationship between power cell reference voltages. On the other hand, it is seen in Fig. 8(b) that the PCC voltage is further distorted at stage 2, due to that the output voltage becomes roughly three-level PWM waveforms. As expected, the output voltage becomes a highly uniform seven-level PWM waveform by applying the decentralized phase-shifting control algorithm. Meanwhile, the PCC voltage as shown in Fig. 8(c) becomes highly sinusoidal due to the reduction of output voltage high-frequency switching harmonic components.

Finally, the harmonic spectra of PCC voltage at three stages are shown in Fig. 9, it is seen that at stage 1 to stage 3, the total

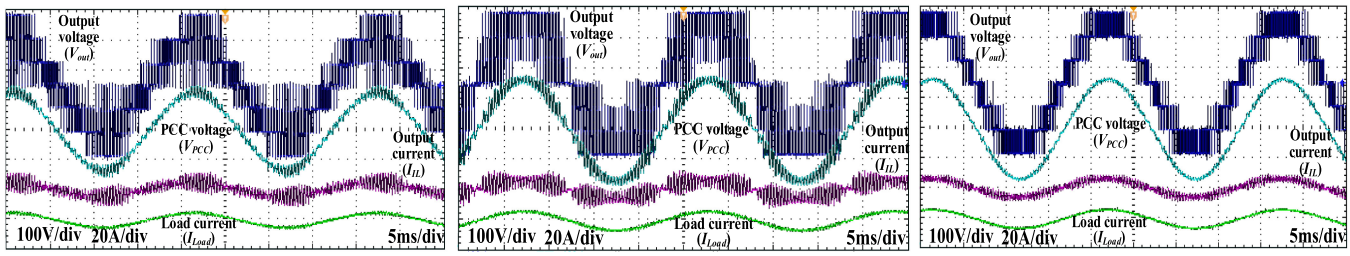

Fig. 8. Output voltage, PCC voltage, output current, and load current performance at three stages. (a) Stage 1. (b) Stage 2. (c) Stage 3.

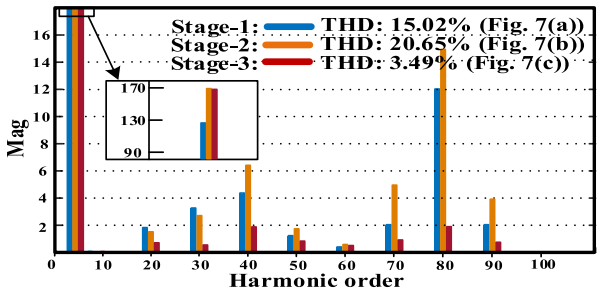

Fig. 9. Harmonic spectra of PCC voltage VPCC at three stages.

harmonic distortions of PCC are 15.02%, 20.65%, and 3.49%, respectively.

IV. Conclusion

In this letter, a decentralized phase-shifting PWM approach is developed for CHB converters. The essence of the proposed method is to use over-sampled output current of each power cell as an inherent synchronizer. With the help of this synchronizer, the digital carrier phase angle at the exact time of fundamental output current zero crossing can be identified. Then, a slow closed-loop digital carrier angle adjustment method is adopted to achieve proper phase-shifting output PWM at the steady state.

References

[1] E. Behrouzian, M. Bongiorno, and R. Teodorescu, "Impact of switching harmonics on capacitor cells balancing in phase-shifted PWM-based cascaded H-bridge STATCOM," *IEEE Trans. Power Electron.*, vol. 32, no. 1, pp. 815–824, Jan. 2017.

[2] A. Moeini and S. Wang, "The state of charge balancing techniques for electrical vehicle charging stations with cascaded H-bridge multilevel converters," in *Proc. IEEE Appl. Power Electron. Conf. Expo.*, San Antonio, TX, USA, 2018, pp. 637–644.

[3] J. He, Y. W. Li, and F. Blaabjerg, "Flexible microgrid power quality enhancement using adaptive hybrid voltage and current controller," *IEEE Trans. Ind. Electron.*, vol. 61, no. 6, pp. 2784–2794, Jun. 2014.

[4] L. Wang, D. Zhang, Y. Wang, B. Wu, and H. S. Athab, "Power and voltage balance control of a novel three-phase solid-state transformer using multilevel cascaded H-bridge inverters for microgrid applications," *IEEE Trans. Power Electron.*, vol. 31, no. 4, pp. 3289–3301, Apr. 2016.

[5] Y. Ko, M. Andresen, G. Buticchi, and M. Liserre, "Power routing for cascaded H-bridge converters," *IEEE Trans. Power Electron.*, vol. 32, no. 12, pp. 9435–9446, Dec. 2017.

[6] L. Liu, H. Li, Y. Xue, and W. Liu, "Decoupled active and reactive power control for large-scale grid-connected photovoltaic systems using cascaded modular multilevel converters," *IEEE Trans. Power Electron.*, vol. 30, no. 1, pp. 176–187, Jan. 2015.

[7] J. He, Y. Li, B. Liang, and C. Wang, "Inverse power factor droop control for decentralized power sharing in series-connected-microconverters-based islanding microgrids," *IEEE Trans. Ind. Electron.*, vol. 64, no. 9, pp. 7444–7454, Sep. 2017.

[8] B. P. McGrath, D. G. Holmes, and W. Y. Kong, "A decentralized controller architecture for a cascaded H-bridge multilevel converter," *IEEE Trans. Ind. Electron.*, vol. 61, no. 3, pp. 1169–1178, Mar. 2014.

[9] *TMS320x2833x, 2823x Enhanced Pulse Width Modulator (ePWM) Module*. Texas Instruments Incorporated, Dallas, TX, USA, Reference Guide, Literature: SPRUG04A, 2008.